Dyes and Pigments 105 (2014) 157–162

Contents lists available at ScienceDirect

Dyes and Pigments

journal homepage: www.elsevier.com/locate/dyepig

Synthesis, structures and photophysical properties of boron–fluorine derivatives based on pyridine/1,8-naphthyridine

Zhensheng Li [a], Xiaojun Lv [a], Yong Chen [a], Wen-Fu Fu [a,b,*]

[a] Key Laboratory of Photochemical Conversion and Optoelectronic Materials, CAS and HKU Joint Laboratory on New Materials, Technical Institute of Physics and Chemistry, Chinese Academy of Sciences, Beijing 100190, PR China
[b] College of Chemistry and Engineering, Yunnan Normal University, Kunming 650092, PR China

ARTICLE INFO

Article history:
Received 7 November 2013
Received in revised form
13 January 2014
Accepted 24 January 2014
Available online 12 February 2014

Keywords:
Boron–fluorine compound
1,8-Naphthyridine
Structures
Solid-state emission
Fluorescence quantum yield
pH sensor

ABSTRACT

Three boron–fluorine complexes **B1**–**B3** containing pyridine/1,8-naphthyridine were synthesized and structurally characterized. Compounds **B1** and **B2** exhibited strong fluorescence in solution and solid state. The solvent-dependent luminous properties and large Stokes shift in solution could be explained by intramolecular charge transfer, which is confirmed by time-dependent density functional theory calculation. The absolute quantum yield of **B1** in powder form reached 0.48 because of inhibiting planar π···π stacking. Single-crystal X-ray diffraction analyses of **B1** and **B2** revealed that weak intermolecular C–H···F and H···π interactions hinder further stacking of π···π dimers, consequently preventing aggregation-induced quenching. Complex **B3**, composed of boron–dipyrromethene and 1,8-naphthyridine fluorophore, had potential applications as a pH ratiometric fluorescent sensor.

1. Introduction

Organoboron complexes are well known as one group of most important fluorescent dyes because of their tunable emission wavelengths [1–3] and high fluorescence quantum yields [4]. In particular, boron dipyrromethene (BODIPY) derivatives have played significant roles in many fields including fluorescent indicators [5], energy-transfer cassettes [6], laser dyes [7], and photodynamic therapy [8]. However, typical BODIPYs suffer from aggregation-induced quenching (ACQ) caused by their small Stokes shift and tight π···π packing in the solid state, which severely limits their applications as electroluminescence materials [9]. Generally, two promising strategies are employed to avoid ACQ in solid state, that is, aggregation-induced emission [10,11] and introduction of bulky groups [12]. Although the methods are effective to enhance solid emission, the energy of excited fluorophores will greatly exhaust *via* nonradiative decay, resulting in low quantum yields in solution [13]. Thus, it is still a challenge to obtain emissive BODIPY derivatives both in solution and solid state.

Naphthyridine derivatives are widely applied as biological probes and assembled supramolecular systems because of its diverse coordination modes and multiple hydrogen-bonded self-assembly ability [14,15]. However, BF_2 core complexes based on 1,8-naphthyridine unit have been little explored. Recently, we have reported a series of emissive 1,8-naphthyridine-BF_2 complexes that exhibit diverse attractive photophysical properties [4,16,17]. Herein, we synthesized three boron complexes **B1**–**B3** containing pyridine/1,8-naphthyridine, and their spectroscopic behaviors were investigated. Both **B1** and **B2** displayed strong emission in the solid state due to weak intermolecular C–H···F and H···π interactions. Although **B3** was not fluorescent in solid state, it exhibited pH-dependent solution-emission spectra by protonation of naphthyridine upon excitation at 330 nm, indicating that **B3** could act as a pH ratiometric fluorescent sensor.

2. Experimental section

2.1. Materials and instrumentations

All starting materials were purchased commercially as reagent grade and used as received unless otherwise mentioned. Dichloromethane was distilled over calcium hydride. The solvents used for spectroscopic measurements were of HPLC grade. 2-(4,5-

* Corresponding author. Key Laboratory of Photochemical Conversion and Optoelectronic Materials, CAS and HKU Joint Laboratory on New Materials, Technical Institute of Physics and Chemistry, Chinese Academy of Sciences, Beijing 100190, PR China.
E-mail address: fuwf@mail.ipc.ac.cn (W.-F. Fu).

http://dx.doi.org/10.1016/j.dyepig.2014.01.022
0143-7208/

diphenyl-1*H*-imidazol-2-yl)pyridine (**L1**) and 2-(pyridin-2-yl)-1*H*-phenanthro[9,10-d]imidazole (**L2**) were synthesized according to the literature methods [18]. 1,8-naphthyridine-2-carbaldehyde was obtained by the previously reported procedure [19].

^{1}H and ^{13}C spectra were recorded on a Bruker Avance 400 spectrometer in $CDCl_3$ at room temperature. Electrospray Ionization (ESI) mass spectra were obtained on a Finnigan LCQ quadrupole ion trap mass spectrometer. UV–Vis absorption spectra were recorded using a Hitachi U-3010 spectrophotometer. Emission and excitation spectra were obtained on a Hitachi F-4500 Fluorescence Spectrophotometer. The fluorescence quantum yields in solution were measured relative to quinine sulfate in 0.1 M sulfuric acid aqueous solution (λ_{ex} = 345 nm, Φ_F = 0.546) at room temperature. The quantum yield was calculated by using Equation (1), where subscripts std denotes standard, Φ is quantum yield, I is the integrated emission intensity, A is the absorbance, and n is the refractive index.

$$\Phi_{sample} = \Phi_{std}\left(A_{std}/A_{sample}\right)\left(I_{sample}/I_{std}\right)\left(n_{sample}/n_{std}\right)^2 \quad (1)$$

Solid-state fluorescence quantum yields were measured using an integrating sphere F-3018 (HORIBA JOBIN YVON) equipped to the Spex 1681 Flurolog-2 Model F111 spectrophotometer. The pH measurements were performed utilizing a Mettler-Toledo FE20K pH meter. Single crystals of **B1** and **B2** suitable for X-ray diffraction were grown by slow evaporation of solutions of the samples in $CHCl_3$. The diffraction data were collected on a Rigaku R-AXIS RAPID IP X-Ray diffractometer using a graphite monochromator with MoKα radiation (λ = 0.071073 nm) at 293 K. The structures were solved by direct methods and refined by full-matrix least-squares methods on all F^2 data (SHELX-97). CCDC-855326 (**B2**) contains the supplementary crystallographic data for this paper [20]. These data can be obtained free of charge from The Cambridge Crystallographic Data Centre via www.ccdc.cam.ac.uk/data_request/cif.

2.2. Synthetic procedures

Synthetic procedures of **B1**–**B3** were depicted in Scheme 1.

2.2.1. Synthesis of BF_2\{2-(4,5-diphenyl-1H-imidazol-2-yl)pyridine\} (*B1*)

At room temperature, triethylamine (2 mL) was added to a stirred mixture of **L1** (297 mg, 1.0 mmol) in dry CH_2Cl_2 (30 mL) under N_2. After 5 min, boron trifluoride etherate (2 mL, 15.7 mmol) was added dropwise. The solution was stirred overnight. The reaction was quenched by adding water (20 mL) and the mixture was extracted with CH_2Cl_2 (2 × 50 mL). The organic phase was dried by anhydrous Na_2SO_4, and concentrated to dryness on a rotary evaporator. The crude product was purified by silica gel column chromatography (CH_2Cl_2/EtOH, 20/1, v/v) to yield **B1** as yellow solid (150 mg, 43%). ^{1}H NMR (400 MHz, $CDCl_3$) 8.45 (d, J = 5.6 Hz, 1H), 8.24–8.16 (m, 1H), 8.09 (d, J = 8.1 Hz, 1H), 7.66–7.60 (m, 2H), 7.60–7.55 (m, 2H), 7.50 (t, J = 6.2 Hz, 1H), 7.42–7.27 (m, 6H) ppm (Fig. S1); ^{13}C NMR (101 MHz, $CDCl_3$) 145.88, 145.58, 145.17, 144.65, 141.30, 134.76, 134.47, 130.80, 128.76, 128.63, 128.38, 128.17, 127.32, 122.73, 117.67 ppm (Fig. S2). ESI-MS m/z calcd. for $C_{20}H_{14}BF_2N_3$ $(M+H)^+$ 346.1; found 346.2. Anal. calcd. for $C_{20}H_{14}BF_2N_3$: C, 69.63; H, 4.09; N, 12.18; found: C, 69.57; H, 4.10; N, 12.22.

2.2.2. BF_2\{2-(pyridin-2-yl)-1H-phenanthro[9,10-d]imidazole\} (*B2*)

The synthesis is analogous to **B1** with **L2** as the starting material. The product was obtained as a brown yellow solid. Yield: 30%. ^{1}H NMR (400 MHz, $CDCl_3$) 8.69 (dd, J = 19.1, 8.9 Hz, 3H), 8.59 (d, J = 5.3 Hz, 1H), 8.47 (d, J = 7.9 Hz, 1H), 8.25 (d, J = 5.9 Hz, 2H), 7.76–7.62 (m, 4H), 7.58 (s, 1H) ppm (Fig. S3); ^{13}C NMR (101 MHz, $CDCl_3$) 146.31, 144.80, 143.53, 141.74, 129.72, 128.86, 127.63, 127.46, 127.29, 126.61, 125.94, 123.74, 123.69, 123.63, 123.49, 123.30, 122.63, 118.78 ppm (Fig. S4); ESI-MS m/z calcd. for $C_{20}H_{12}BF_2N_3$ $(M+H)^+$ 344.1; found 344.2. Anal. calcd. for $C_{20}H_{12}BF_2N_3$: C, 70.03; H, 3.52; N, 12.25; found: C, 70.10; H, 3.55; N, 12.20.

2.2.3. 8-(1,8-naphthypridine)-1,3,5,7-tetramethyl-4,4-difluoroboradiazaindacene (*B3*)

1,8-Naphthyridine-2-carbaldehyde (370 mg, 2.3 mmol) was dissolved in dry CH_2Cl_2 (200 mL). 2,4-Dimethylpyrrole (456 mg, 4.8 mmol) and one drop of trifluoroacetic acid were added under N_2 atmosphere. The mixture was stirred at room temperature in the dark for 3 h. After oxidation with 2,3-dichloro-5,6-dicyano-p-benzoquinone (DDQ) (1.01 g, 2.3 mmol), triethylamine (TEA) (4 mL) and $BF_3{\cdot}Et_2O$ (5 mL) were added dropwise to the mixture. The reaction solution was stirred for another 3 h, and the brown mixture was washed with water and brine, dried over anhydrous magnesium sulfate and concentrated at reduced pressure. The crude product was purified by silica-gel column chromatography (petroleum/EtOAc = 10:1, v/v) to yield **B3** as red solid, 130 mg, yield 15%. ^{1}H NMR (400 MHz, $CDCl_3$) δ 9.24 (d, J = 2.3 Hz, 1H), 8.38 (d,

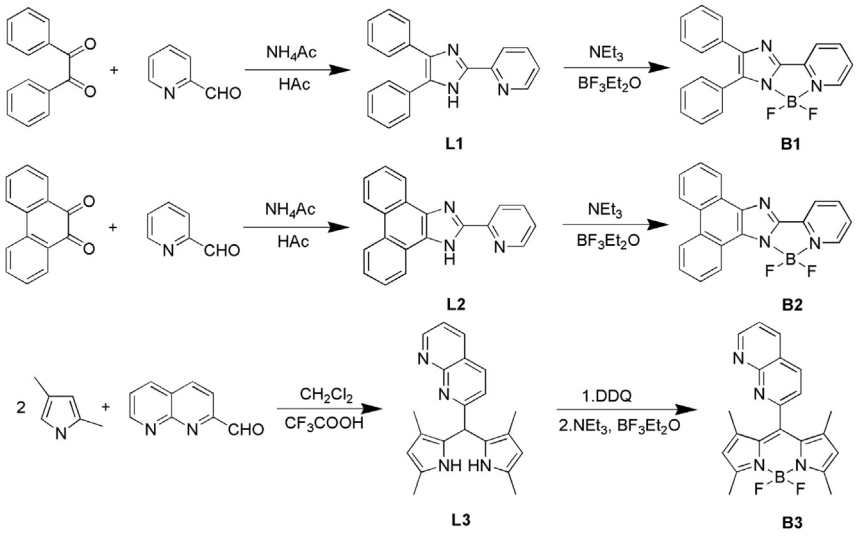

Scheme 1. Synthetic procedures and chemical structures of **B1**–**B3**.

J = 8.2 Hz, 1H), 8.32 (dd, J = 8.2, 1.8 Hz, 1H), 7.67–7.60 (m, 2H), 5.98 (s, 2H), 2.58 (s, 6H), 1.23 (s, 6H) ppm (Fig. S5). ESI-MS m/z calcd. for $C_{21}H_{19}BF_2N_4$ $(M+H)^+$ 377.1; found 377.2. Anal. calcd. for $C_{21}H_{19}BF_2N_4$: C, 67.06; H, 5.09; N, 14.90; found: C, 67.13; H, 5.06; N, 14.95.

3. Result and discussion

3.1. Single X-ray crystallography

By slow evaporation of the samples in $CHCl_3$, only single crystals of **B1** and **B2** suitable for X-ray diffraction analysis were obtained. Both compounds were crystallized in space group $P2_1/c$. As shown in Fig. 1, **B1** and **B2** had similar crystal structures, exhibiting a slightly distorted tetrahedral geometry around boron atoms. The bond lengths of B1–N1 and B1–N2 were 1.616(2) and 1.539(2) Å in the structure of **B1**, respectively, and these corresponding bond lengths for **B2** were 1.611(4) and 1.541(4) Å. The coordination of boron with nitrogen atoms forced the related imidazole and pyridine rings in both structures to lie in a plane. In **B1**, because of the steric hindrance among the aromatic rings, the dihedral angles between imidazole–pyridine plane and two phenyl rings were 7.1° and 37.5°, respectively. In contrast, the two terminal phenyl rings in **B2** were fused together with imidazole moiety to form as a phenanthro[9,10-d]-imidazole group, the whole molecular were therefore highly planar with a small average deviation of 0.0295 Å.

Both compounds contain conjugated aromatic system, thus they could form dimers by π···π interactions. Furthermore, the dimers were further extended along crystallographic b axis through weak C–H···F and H···π contacts instead of π···π interactions (Fig. 2). In the structure of **B1**, the π···π stacking area decreased due to steric hindrance caused by two lateral twisted phenyl rings. For **B2**, the $CHCl_3$ molecule interacts with the host molecule by way of C–H···N hydrogen bond.

3.2. Spectroscopic properties

The spectral properties of **B1**–**B3** in various solvents and solid state were examined. The data were summarized in Table 1. **B1** and **B2** exhibited multiple absorption bands in $CHCl_3$, and the lowest-energy absorption maxima at 414 nm for **B1** and 430 nm for **B2** were attributed to S_0–S_1 transition. In comparison with that of **B1**, the lower-energy absorption of **B2** is ascribed to the enlarged π-conjunction system lowering the transition energy (Fig. 3). The molar absorption coefficient for **B2** was much larger than that of **B1**, because the twisted phenyl rings of **B1** did not facilitate electrons transition. Compound **B3** exhibited an intense absorption band at 509 nm and moderate absorptions at 338 nm in $CHCl_3$. The former was typical for the BODIPY dyes, attributed to the 0–0 vibrational band of the S_0–S_1 transition, while the latter were associated with 1,8-naphthyridine unit [14].

The solution emission maxima of **B1** and **B2** in $CHCl_3$ were located at 520 nm and 522 nm, respectively. The Stokes shift of **B1** was up to 106 nm, which was 14 nm larger than that of **B2**. And the fluorescence quantum yield of **B1** (Φ = 0.23) was a little lower than that of **B2** (Φ = 0.30). The results were not surprising because the phenyl rings of **B1** appended to the imidazole ring could rotate around the C–C bond, which reduced the energy of the excited state even though the rotation was limited by steric hindrance. However, this did not occur in the fused ring system in **B2**. The Stokes shift of **B3** was only 15–18 nm in solution, which was usual for 8-substituted BODIPY derivatives (Fig. 3).

Interestingly, both the absorption and emission spectra of **B1** and **B2** were solvent-dependent (Fig. 4 and Fig. S6). With solvent polarity increasing, the lowest-energy absorption bands were marked blue-shift. For example, the absorption peak of **B2** was observed at 447 nm in hexane, while the corresponding peak appeared at 403 nm in acetonitrile. Similar behaviors were also observed for compound **B1**. The observed negative solvatochromism indicates that the energy level of the ground state decreases more significantly than that of excited state with increasing solvent polarity, making energy gap larger. The solvent-dependent behaviors indicated the S_0–S_1 absorption bands with intramolecular charge transfer (ICT) characteristics [21].

Diphenyl-imidazole or phenanthro-imidazole substituents as electron-donating groups, along with a BF_2 core and pyridine electron-deficient moieties, resulted in a "push–pull" system [17]. Photoexcitation of such a system would generate large dipolar moments affected significantly by environmental polarity. In addition, Emission spectra of **B1** and **B2** measured in polar solvents displayed bathochromic shifts with low fluorescence yields [22] and increased Stokes shifts in polar solvent, which further confirmed the ICT mechanism. The spectra of **B2** contained well-resolved vibrational structure (Fig. 4) in hexane, which disappeared gradually with increasing solvent polarity as the vibration was restrained by polar molecules.

Compounds **B1** and **B2** were highly fluorescent in solid state. By an integrating sphere, the absolute fluorescent quantum yields for **B1** and **B2** in powder form were estimated to be 0.48 and 0.21, respectively. **B1** exhibited more intense solid-state fluorescence than **B2** due to the unfused phenyl rings considerably decreasing stacking area, which was confirmed by X-ray single crystal analysis. Notably, the maximum emission wavelengths of **B1** and **B2** had no obvious difference whatever in solution and in solid powder, which indicated the fused phenyl rings have less effect on the emission spectra than fused thiophene system [23]. As expected, **B3** did not

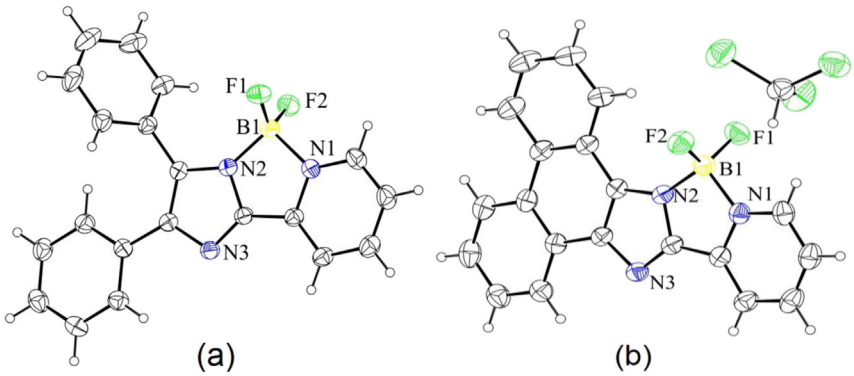

Fig. 1. Crystal structures of **B1** (a) and **B2** (b).

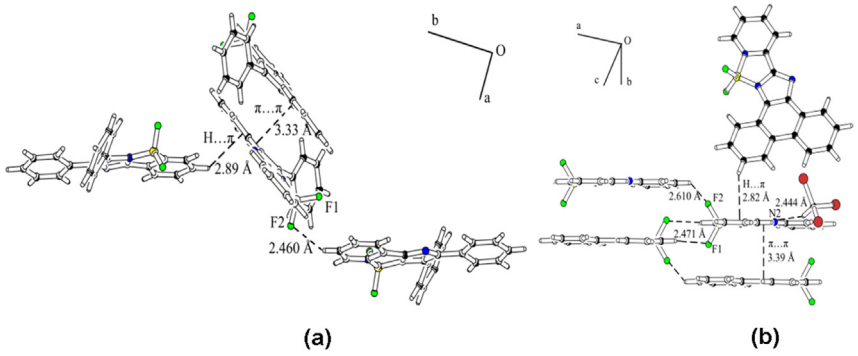

Fig. 2. Weak intermolecular interactions in **B1** (a) and **B2** (b).

Table 1
Spectroscopic properties of **B1**–**B3** in various solvent and in solid state.

Dyes	Media	λ_{abs}/nm	ε_{max} ($dm^3\ mol^{-1}\ cm^{-1}$)	λ_{em}/nm	Stokes shift/nm	Φ_F
B1	Hexane	428	14,600	510	82	0.22
	CH_2Cl_2	408	14,200	528	120	0.15
	$CHCl_3$	414	15,000	520	106	0.23
	CH_3OH	391	13,500	525	134	0.12
	CH_3CN	393	12,100	543	150	0.10
	Solid	–	–	509	–	0.48
B2	Hexane	447	15,500	507	67	0.95
	CH_2Cl_2	421	19,600	526	105	0.32
	$CHCl_3$	430	21,000	522	92	0.30
	CH_3OH	404	20,000	531	127	0.14
	CH_3CN	403	20,000	527	124	0.08
	Solid	–	–	502	–	0.21
B3	Hexane	506	44,600	524	18	0.08
	CH_2Cl_2	506	60,000	522	16	0.06
	$CHCl_3$	509	55,000	527	16	0.07
	CH_3OH	503	55,800	521	18	0.16
	CH_3CN	501	55,200	516	15	0.04

display any fluorescence in the solid state possibly due to π···π interaction [24].

3.3. pH dependent fluorescence

It has been previously reported that the fluorescence of BF_2-core compounds could be tuned by protonation of imidazole/pyridine [25,26]. Unfortunately, the presented compounds **B1** and **B2** were unstable in the low pH value media due to the imidazole was protonated. In the range of pH values 2.1–4.9, the absorbance of naphthyridine moiety in **B3** increased with an isobestic point at 300 nm, whereas the main absorption band attributed to BODIPY core did not show obvious changes. Upon excitation at 330 nm, **B3** exhibited two main emission bands at 521 nm and 365 nm in CH_3OH/H_2O (1:1 v/v) (Fig. 5, Figs. S7 and S8). The former was typical fluorescence for the BODIPY dyes, and the latter was associated with 1,8-naphyridine unit. Addition of H^+ to **B3** in CH_3OH/H_2O solution, the intensity of emission peak at 521 nm decreased while the one at 365 nm increased significantly when the 1,8-naphthyridine unit was protonated. The results revealed that the oxidative photoinduced electron transfer from the excited BODIPY to the electron-deficient 1,8-naphthyridine unit, resulting in fluorescence from BODIPY quenching [27,28]. The ration of the fluorescent intensities at 365 nm and 521 nm (I_{365}/I_{521}) increased from 0.05 to 4.50. The results indicate that **B3** can be considered as a ratiometric pH sensor.

3.4. Time-dependent density functional theory calculations

To gain further insight into the observed spectroscopic behavior of **B1** and **B2**, time-dependent density functional theory calculations were performed on the dyes using the Gaussian 09 package [29]. The geometrical structures for the ground and lowest singlet excited states of the compounds were optimized at the TD-CAM-B3LYP/6-31-G(d) level [30]. The character of singly occupied orbitals of the $S_0 \rightarrow S_1$ transitions of **B1** and **B2** were shown in Fig. 6. The transitions of **B1** and **B2** both originated from a π orbital mainly localized on a 4,5-diphenyl-imidazol or phenanthro[9,10-d]imidazole unit to a π* orbital localized on the pyridine moiety. The electron redistribution resulted in the considerable dipole moment changes of −9.12 D for **B1** and −9.19 D for **B2** along the *x* direction (from the left benzene

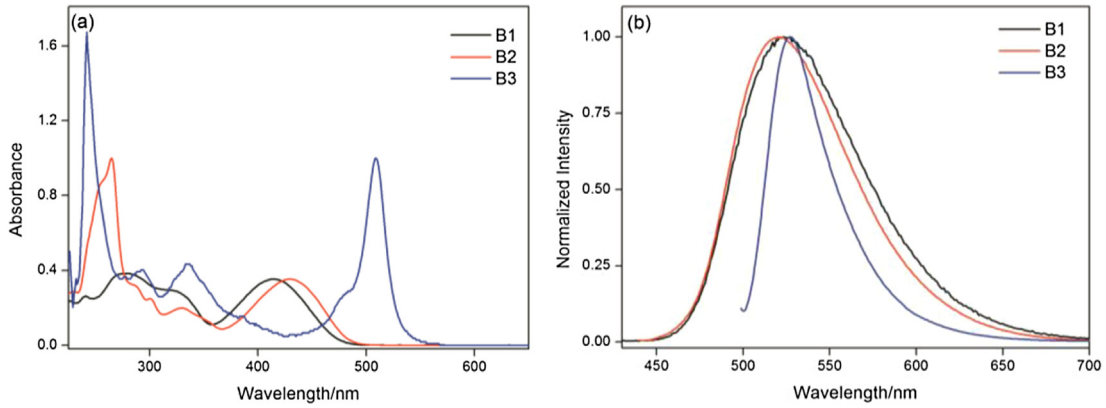

Fig. 3. Absorption (a) and emission (b) spectra of **B1**–**B3** in $CHCl_3$.

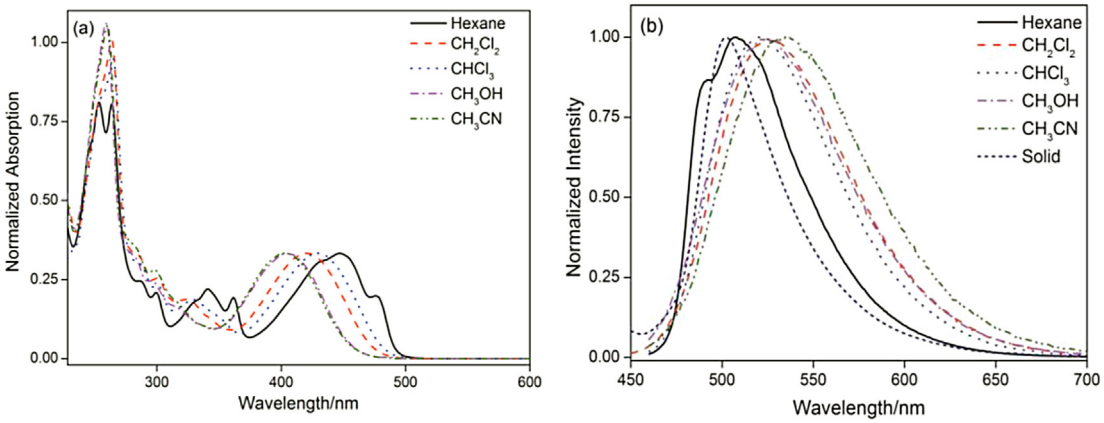

Fig. 4. The Absorption (a) and emission (b) spectra of compound **B2** in different organic solvent and solid state.

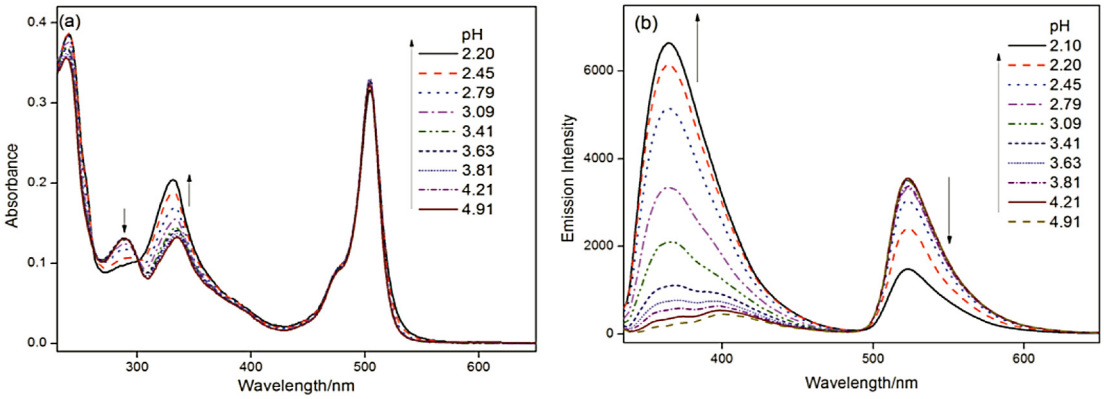

Fig. 5. The effects of pH values on the absorption (a) and emission (b) spectra of **B3** (5 μM, λ_{ex} = 330 nm).

ring to the pyridine unit). This indicated that an efficient intramolecular charge transfer process could be responsible for large Stoke shifts and solvatochromism of these compounds. The vertical excitation energies in the gas phase were calculated to be 373 nm for **B1** and 380 nm for **B2**, which is a slight blue shift compared with the experimental absorption spectra in solution. However, the calculated trends of both complexes were in good agreement with those obtained experimentally.

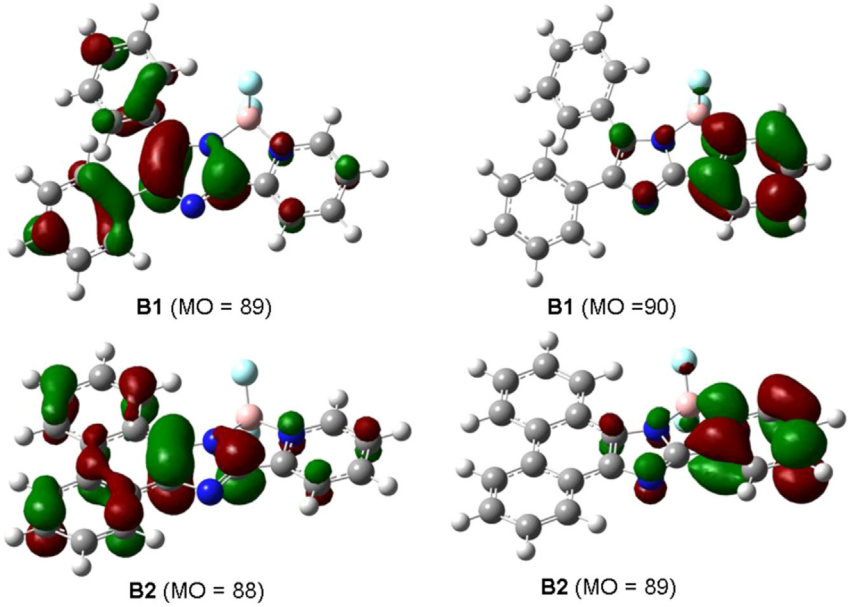

Fig. 6. The singly occupied molecular orbitals of the $S_0 \rightarrow S_1$ transitions of compounds **B1** and **B2**.

4. Conclusions

In summary, we have developed a series of BF_2 core complexes containing pyridine/naphthyridine with intense solid-state fluorescence. The ICT process leads to large Stokes shifts and solvent-dependent photophysical properties for **B1** and **B2**. The intense solid emissions of **B1** and **B2** indicate that the weak intermolecular interactions could inhibit aggregation-induced quenching, which is instructive for developing solid-state luminescent materials. **B3** does not show similar spectroscopic behaviors, but it displays about 90-fold fluorescence ratio change upon protonated in CH_3OH/H_2O, which indicates that the compound could serve as a pH ratiometric fluorescent sensor.

Acknowledgments

This work was financially supported by the Ministry of Science and Technology (2013CB834804, 2012DFH40090). We thank the Natural Science Foundation of China (NSFC Grant Nos. 21071123, 21273257 and U1137606), and CAS-Croucher Funding Scheme for Joint Laboratories, Yunnan Key Project (2010CC007) and Program for Changjiang Scholars and Innovative Research Team in University (IRT0979) for financial support.

Appendix A. Supplementary data

Supplementary data related to this article can be found at http://dx.doi.org/10.1016/j.dyepig.2014.01.022.

References

[1] Liu QD, Mudadu MS, Thummel R, Tao Y, Wang S. From blue to red: syntheses, structures, electronic and electroluminescent properties of tunable luminescent N,N chelate boron complexes. Adv Funct Mater 2005;15:143–54.
[2] Umezawa K, Nakamura Y, Makino H, Citterio D, Suzuki K. Bright, color-tunable fluorescent dyes in the visible-near-infrared region. J Am Chem Soc 2008;130:1550–1.
[3] Santra M, Moon H, Park MH, Lee TW, Kim YK, Ahn KH. Dramatic substituent effects on the photoluminescence of boron complexes of 2-(benzothiazol-2-yl) phenols. Chem Eur J 2012;18:9886–93.
[4] Li HJ, Fu WF, Li L, Gan X, Mu WH, Chen WQ, et al. Intense one- and two-photon excited fluorescent Bis(BF_2) core complex containing a 1,8-naphthyridine derivative. Org Lett 2010;12:2924–7.
[5] Boens N, Leen V, Dehaen W. Fluorescent indicators based on BODIPY. Chem Soc Rev 2012;41:1130–72.
[6] Benstead M, Mehl GH, Boyle RW. 4,4′-Difluoro-4-bora-3a,4a-diaza-s-indacenes (BODIPYs) as components of novel light active materials. Tetrahedron 2011;67:3573–601.
[7] Zhang D, Martin V, Garcia-Moreno I, Costela A, Perez-Ojeda ME, Xiao Y. Development of excellent long-wavelength BODIPY laser dyes with a strategy that combines extending π-conjugation and tuning ICT effect. Phys Chem Chem Phys 2011;13:13026–33.
[8] Kamkaew A, Lim SH, Lee HB, Kiew LV, Chung LY, Burgess K. BODIPY dyes in photodynamic therapy. Chem Soc Rev 2013;42:77–88.
[9] Hong Y, Lam JWY, Tang BZ. Aggregation-induced emission. Chem Soc Rev 2011;40:5361–88.
[10] Yang Y, Su X, Carroll CN, Aprahamian I. Aggregation-induced emission in BF_2-hydrazone (BODIHY) complexes. Chem Sci 2012;3:610–3.
[11] Zhang ZY, Xu B, Su JH, Shen LP, Xie YS, Tian H. Color-tunable solid-state emission of 2,2′-biindenyl-based. Angew Chem Int Ed 2011;50:11654–7.
[12] Lu H, Wang Q, Gai L, Li Z, Deng Y, Xiao X, et al. Tuning the solid-state luminescence of BODIPY derivatives with bulky arylsilyl groups: synthesis and spectroscopic properties. Chem Eur J 2012;18:7852–61.
[13] Kubota Y, Tanaka S, Funabiki K, Matsui M. Synthesis and fluorescence properties of thiazole-boron complexes bearing a β-ketoiminate ligand. Org Lett 2012;14:4682–5.
[14] Chen Y, Fu WF, Li JL, Zhao XJ, Ou XM. Conformation impact on spectral properties of bis(5,7-dimethyl-1,8-naphthyridin-2-yl)amine and its Zn^{II} complex. New J Chem 2007;31:1785–8.
[15] de Greef TF, Ercolani G, Ligthart GBWL, Meijer EW, Sijbesma RP. Influence of selectivity on the supramolecular polymerization of AB-type polymers capable of both A···A and A···B interactions. J Am Chem Soc 2008;130:13755–64.
[16] Quan L, Chen Y, Lv XJ, Fu WF. Aggregation-induced photoluminescent changes of naphthyridine-BF_2 complexes. Chem Eur J 2012;18:14599–604.
[17] Wu YY, Chen Y, Gou GZ, Mu WH, Lv XJ, Du ML, et al. Large stokes shift induced by intramolcular charge transfer in N,O-chelated naphthyridine-BF_2 complexes. Org Lett 2012;14:5226–9.
[18] Eseola AO, Zhang M, Xiang JF, Zuo W, Li Y, Woods JAO, et al. Synthesis and characterization of nickel(II) complexes bearing 2-(imidazol-2-yl)pyridines or 2-(pyridin-2-yl)phenanthroimidazoles/oxazoles and their polymerization of norbornene. Inorg Chim Acta 2010;363:1970–8.
[19] Vu C, Walker DD, Wells J, Fox S. Elaboration of 1,8-naphthyridine-2,7-dicarboxaldehyde into novel 2,7-dimenthylimine derivatives. J Heterocycl Chem 2002;39:829–32.
[20] The main work of the article has been completed in 2011. In 2012, the authors became aware of a report where compound **B1** was prepared by Mao M, Xiao S, Li J, Zou Y, Zhang R, Pan J, et al. Solid-emissive boron-fluorine derivatives with large Stokes shift Tetrahedron 2012;68:5037–41. In present work, the effect of fused phenyl rings on spectral characteristics of **B1** and **B2** are fully compared.
[21] Zhang JC, Wang DY. Modern photochemistry. Beijing: Industry Press Journal; 2006. pp. 22–4.
[22] Wu SK. The problem on photophysics and photochemistry of organic compounds possessing ability of fluorescence emission. Prog Chem 2005;17:15–39.
[23] Wong HL, Wong WT, Yam VWW. Photochromic thienylpyridine-bis(alkynyl) borane complexes: toward readily tunable fluorescence dyes and photoswitchable materials. Org Lett 2012;14:1862–5.
[24] Arroyo IJ, Hu R, Merino G, Tang BZ, Peña-cabrera Eduardo. The smallest and one of the brightest efficient preparation and optical description of the parent borpndipyrromethane system. J Org Chem 2009;74:5719–22.
[25] Eseola AO, Li W, Adeyemi OG, Obi-Egbedi NO, Woods JAO. Hemilability of 2-(1H-imidazol-2-yl)pyridine and 2-(oxazol-2-yl)pyridine ligands: imidazole and oxazole ring Lewis basicity, Ni(II)/Pd(II) complex structures and spectra. Polyhedron 2010;29:1891–901.
[26] Bartelmess J, Weare WW, Latortue N, Duong C, Jones DS. *meso*-Pyridyl bodipys with tunable chemical, optical and electrochemical properties. New J Chem 2013;37:2663–8.
[27] Wang YW, Li M, Shen Z, You XZ. *meso*-Pyridine substituted boron-dipyrromethenen (BDP) dyes as a pH probe: synthesis, crystal structure and spectroscopic properties. Chin J Inorg Chem 2008;24:1247–52.
[28] Chen Y, Wang H, Wan L, Bian Y, Jiang J. 8-Hydroxyquinoline-substituted boron-dipyrromethene compounds: synthesis, structure, and OFF-ON-OFF type of pH-sensing properties. J Org Chem 2011;76:3774–81.
[29] Frisch MJ, Trucks GW, Schlegel HB, Scuseria GE, Robb MA, Cheeseman JR, et al. Gaussian 09, revision C.01. Wallingford CT: Gaussian, Inc.; 2010.
[30] Yanai T, Tew DP, Handy NC. A new hybrid exchange-correlation functional using the coulomb-attenuating method (CAM-B3LYP). Chem Phys Lett 2004;393:51–7.